J. Fluid Mech. (1972), *vol.* 55, *part* 3, *pp.* 529–543
Printed in Great Britain

A class of exact, time-dependent, free-surface flows

By M. S. LONGUET-HIGGINS
Department of Applied Mathematics and Theoretical Physics, University of Cambridge, and National Institute of Oceanography, Wormley, Surrey

(Received 18 December 1969 and in revised form 20 July 1972)

Attention is drawn to a class of inviscid irrotational flows which satisfy the conditions at a time-dependent free surface exactly. The flows are related to the ellipsoids of Dirichlet (1860).

Depending on a parameter P, the cross-section may take the form of a variable ellipse ($P < 0$), a hyperbola ($P > 0$) or a pair of parallel lines ($P = 0$). The elliptical case was investigated both theoretically and experimentally by Taylor (1960). The hyperbolic case ($P > 0$) is remarkable in that the flow develops a singularity when the angle between the asymptotes approaches a right-angle. It is suggested that this solution represents a possible instability near the crest of a standing gravity wave of large amplitude.

In the intermediate case ($P = 0$) the solution describes an open-channel flow in which the fluid filaments are stretched uniformly in a horizontal direction. The latter flow is demonstrated experimentally.

1. Introduction

Exact solutions of the time-dependent equations of motion for a non-viscous fluid with a free surface are quite rare. One class of motions known since the last century is the ellipsoids of Dirichlet (1860), in which a rotating, gravitating mass of fluid, of constant density and vorticity, is contained within a closed ellipsoidal surface, which deforms continuously with time. The solution of the three-dimensional problem has been derived concisely by Lamb (1932, § 382).

A two-dimensional form of these motions was rediscovered by Taylor (1960) in the course of an experimental and theoretical study of the form of a jet issuing from an elliptical orifice.

More recently the present author (1969), who was interested in the form of a standing gravity wave of maximum amplitude, inadvertently discovered a hyperbolic form of the same solution. Unlike the elliptical case, however, the hyperbolic solution shows the interesting feature of a pressure singularity, or shock, at the instant when the angle between the asymptotes becomes equal to a right-angle. Though not necessarily describing the limiting form of a standing gravity wave, the hyperbolic solution may very well describe an instability near the wave crest, or the time-dependent behaviour of a jet impinging on a plane wall.

It is the description of the hyperbolic flow which is the main purpose of the present paper. Section 2 outlines a general approach to the problem of time-dependent free-surface flows. The most general two-dimensional solution with constant rate of strain is derived in § 3. It is seen to depend upon two dimensionless parameters P and Q, governing respectively the time and length scales of the motion. The elliptical case ($P < 0$) is described in § 4, in a form rather different from that given by Taylor (1960). The description of the hyperbolic case is given in § 5, followed by a discussion of its applicability to the standing wave.

The intermediate case ($P = 0$) is also of interest (§ 6). This describes a flow bounded by two parallel plane surfaces, which approach one another. The intervening fluid is ejected in such a way that any given particle travels outwards with constant velocity. The flow is related to a well-known open-channel flow but is exact, not being dependent on the shallow-water approximation or the hydrostatic assumption. The flow is verified in a simple experiment, described in § 8.

2. The general problem

We seek a potential $\phi(x, y, t, z)$ satisfying Laplace's equation

$$\nabla^2\phi = 0, \tag{2.1}$$

and a pressure function $p(x, y, z, t)$ related to ϕ by Bernoulli's theorem:

$$\frac{p}{\rho} = -\frac{\partial\phi}{\delta t} - \tfrac{1}{2}(\nabla\phi)^2 - V, \tag{2.2}$$

where V is the gravitational potential, so that there exists a free surface on which the pressure vanishes:

$$p = 0. \tag{2.3}$$

Since the surface moves with the fluid we must have also

$$\frac{Dp}{Dt}, = \frac{\partial p}{\partial t} + \nabla\phi \, . \, \nabla p, = 0 \tag{2.4}$$

on the same surface. An arbitrary function of the time, which is sometimes added to (2.2), is considered as being absorbed into ϕ.

3. A two-dimensional, gravity-free solution

Let us write
$$\phi = \tfrac{1}{2}A(x^2 - y^2) - \int f\, dt, \tag{3.1}$$

where A and f are functions of the time, to be determined. The components u and v of the velocity in the x and y directions are given by

$$u = Ax, \quad v = -Ay. \tag{3.2}$$

This is a simple, two-dimensional shear flow, as illustrated in figure 1. The flow is symmetrical about both the x axis and the y axis, the instantaneous streamlines being rectangular hyperbolae. The instantaneous streamlines in this particular flow coincide with the particle trajectories.

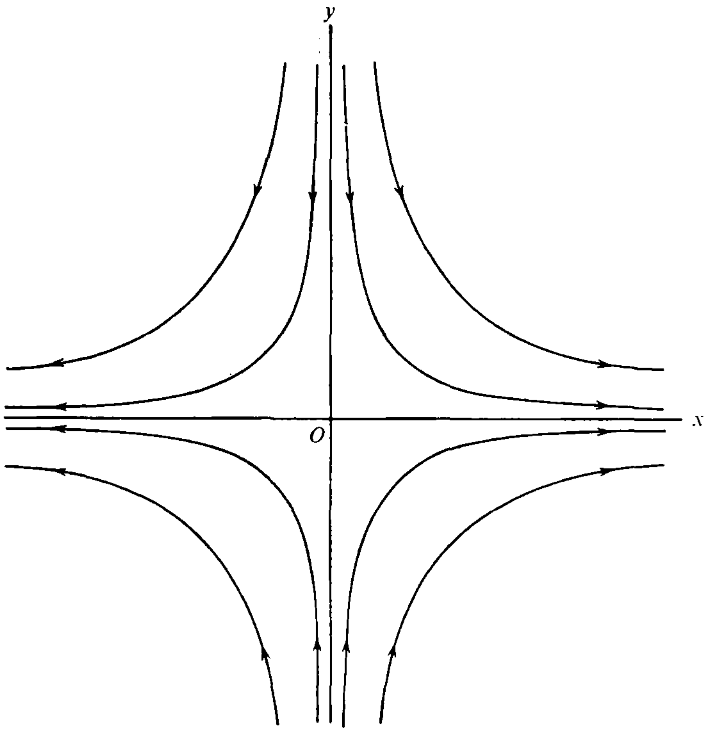

FIGURE 1. The pattern of streamlines corresponding to the velocity potential of equation (3.1), when $A > 0$. (When $A < 0$ the flow is reversed.)

Gravity being neglected, we may write $V = 0$ in (2.2), so that the pressure p is given by

$$p/\rho = -\tfrac{1}{2}(\dot{A} + A^2)\,x^2 + \tfrac{1}{2}(\dot{A} - A^2)\,y^2 + f, \tag{3.3}$$

where a dot denotes partial differentiation with respect to t. Hence the rate of change of p following the motion is given by

$$\frac{1}{\rho}\frac{Dp}{Dt} = -\tfrac{1}{2}(\ddot{A} + 4A\dot{A} + 2A^3)\,x^2 + \tfrac{1}{2}(\ddot{A} - 4A\dot{A} + 2A^3)y^2 + \dot{f}. \tag{3.4}$$

If $p = 0$ and $Dp/Dt = 0$ are to represent the same surface, the corresponding terms in (3.3) and (3.4) must be proportional. So we must have

$$\frac{\ddot{A} + 4A\dot{A} + 2A^3}{\dot{A} + A^2} = \frac{\ddot{A} - 4A\dot{A} + 2A^3}{\dot{A} - A} = \frac{\dot{f}}{f}. \tag{3.5}$$

The terms in A alone give

$$A\ddot{A} - 4\dot{A}^2 + 2A^4 = 0. \tag{3.6}$$

Multiplying each side by $2\dot{A}/A^9$ and integrating we obtain

$$\frac{\dot{A}^2}{A^8} - \frac{1}{A^4} = P, \tag{3.7}$$

a constant, so that

$$\dot{A}^2 = A^4(1 + PA^4). \tag{3.8}$$

Hence
$$t = \pm \int \frac{dA}{A^2(1+PA^4)^{\frac{1}{2}}}. \tag{3.9}$$

Now each ratio in (3.5) is equal to the ratio of the *differences* of any pair of numerators to the *differences* of the denominators. Thus we have
$$\dot{f}/f = 4A\dot{A}/A^2 = 4\dot{A}/A, \tag{3.10}$$
which has the solution
$$f = \tfrac{1}{2}QA^4, \tag{3.11}$$
where Q is a constant.

Hence altogether from (3.3)
$$2p/\rho = -(\dot{A}+A^2)x^2+(\dot{A}-A^2)y^2+QA^4, \tag{3.12}$$
the function $A(t)$ being given inversely by (3.9). The free surface $p = 0$ is an ellipse or a hyperbola according as the coefficients of x^2 and y^2 are of the same or opposite sign, that is according as
$$A^4 \gtrless \dot{A}^2, \quad P \lessgtr 0. \tag{3.13}$$
We shall take these two cases separately.

4. The elliptical case ($P < 0$)

Write
$$(-P)^{\frac{1}{4}} = M > 0, \tag{4.1}$$
so that when $0 < MA < 1$ equation (3.9) becomes
$$t = \int_A^{M^{-1}} \frac{dA}{A^2(1-M^4A^4)^{\frac{1}{2}}}, \tag{4.2}$$
the constant of integration being suitably chosen. The substitution
$$MA = \cos\alpha \quad (0 < \alpha < \tfrac{1}{2}\pi) \tag{4.3}$$
leads to
$$t = M\int_0^{\alpha} \frac{d\theta}{\cos^2\theta(2-\sin^2\theta)^{\frac{1}{2}}}. \tag{4.4}$$
This integral may be expressed in terms of the Legendre elliptic integrals
$$\left.\begin{aligned} E(\alpha,k) &= \int_0^{\alpha}(1-k^2\sin^2\theta)^{\frac{1}{2}}\,d\theta, \\ F(\alpha,k) &= \int_0^{\alpha}\frac{d\theta}{(1-k^2\sin^2\theta)^{\frac{1}{2}}}, \end{aligned}\right\} \tag{4.5}$$
tabulated, for example, by Byrd & Friedman (1954). In fact
$$t = 2^{\frac{1}{2}}M[\tan\alpha\,(1-\tfrac{1}{2}\sin^2\alpha)^{\frac{1}{2}} - E(\alpha, 2^{\frac{1}{2}}) + \tfrac{1}{2}F(\alpha, 2^{\frac{1}{2}})]. \tag{4.6}$$

Using α as a parameter, A may now be plotted as a function of t as in figure 2, for fixed values of M. When $t < 0$ the solution found by reflexion in the line $t = 0$ is analytically continuous with the solution for $t > 0$. The limiting case $M = 0$, however, requires special treatment (see below). In general A attains a maximum value M^{-1} at time $t = 0$, as can be seen also from (4.2). When on the other hand $t \to \infty$ then $A \to 0$, and from (4.2) $A \sim t^{-1}$.

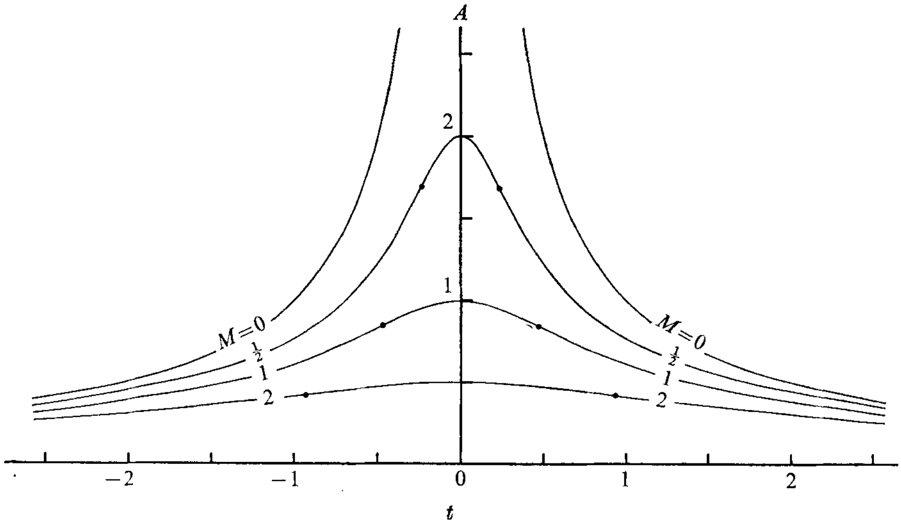

FIGURE 2. The function $A(t)$ when $P < 0$, giving the velocity at a fixed point as a function of the time t. Only the curves for $A > 0$ are shown. Those for $A < 0$ are obtained by reflexion in the t axis.

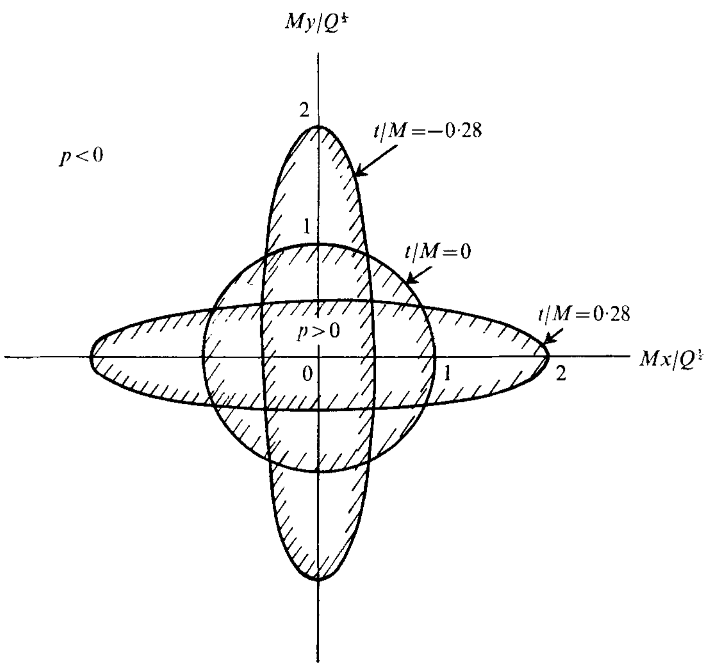

FIGURE 3. Successive configurations of the free surface when $P < 0$ (and $A > 0$). The shading shows the regions where the pressure is positive.

Between $t = \pm\infty$ the sign of A remains the same (positive in figure 2), so that the flow at any given point remains constant in direction. The curve of $A(t)$ has points of inflexion ($\ddot{A} = 0$) where $PA^4 = -\frac{1}{2}$, that is to say where

$$MA = 2^{-\frac{1}{4}} = 0{\cdot}8409\ldots. \tag{4.7}$$

The free surface $p = 0$ may be written in the usual form for an ellipse:

$$\frac{x^2}{a^2}+\frac{y^2}{b^2} = 1, \tag{4.8}$$

where a and b are the lengths of the semi-axes, given by

$$a^2 = \frac{QA^4}{A^2+\dot{A}}, \quad b = \frac{QA^4}{A^2-\dot{A}}. \tag{4.9}$$

Since $A^2 > |\dot{A}|$ by (3.13) it is clear that for a real free surface to exist Q must be positive. Also from (4.9) we have

$$a^2b^2 = \frac{Q^2A^8}{A^4-\dot{A}^2} = -\frac{Q}{P} \tag{4.10}$$

by the differential equation (3.8). Hence the product of the semi-axes of the ellipse is equal to $(-Q/P)^{\frac{1}{2}}$, a constant, as we would expect from continuity, πab being equal to the cross-sectional area.

We also have

$$a^2 = \frac{Q}{M^4}\frac{A^2-\dot{A}}{A^4}, \quad b^2 = \frac{Q}{M^4}\frac{A^2+\dot{A}}{A^4}, \tag{4.11}$$

and so if $\dot{A}$ is expressed in terms of A,

$$a^2 = \frac{Q}{M^2}\frac{1\pm(1-M^4A^4)^{\frac{1}{2}}}{M^2A^2}, \quad b^2 = \frac{Q}{M^2}\frac{1\mp(1-M^4A^4)^{\frac{1}{2}}}{M^2A^2} \tag{4.12}$$

according as $t \gtrless 0$. When $t = 0$, then a and b are both equal to $Q^{\frac{1}{2}}/M$, and the cross-section is circular. When $t > 0$ the ellipse is elongated in the x direction and when $t < 0$ it is elongated in the y direction, as shown in figure 3.

It will be seen from (3.12) that the pressure p is a maximum at the centre of the ellipse, at which point the velocity is zero, and that in general the pressure increases towards the centre. This suggests that the flow may be stable provided that the fluid is contained within the ellipse. The corresponding flow for an elliptical cavity, when the fluid is outside the ellipse, is probably unstable.

A further property of the flow is that all surfaces of constant pressure ($p = p_0$) are similar to the free surface $p = 0$, but that these do not move with the fluid unless we assume that p_0 is not constant but varies in time like A^4.

The pressure at the centre of the ellipse $(x, y) = (0, 0)$ is given by

$$p/\rho = \tfrac{1}{2}QA^4. \tag{4.13}$$

This was compared by Taylor (1960) with the pressure measured at the centre of a jet issuing from an elliptical orifice in a vertical wall, with very good agreement (see Taylor 1960, figure 5).

Taylor's derivation of (4.13) differs from the one given here, the time dependence being expressed in the form of an integral, which is then expanded as an infinite series. It may be noted that the infinite series

$$1-\frac{1}{2.3}+\frac{1}{8.7}-\frac{1}{16.11}+\dots,$$

which is summed numerically by Taylor is equal to

$$2E(\tfrac{1}{4}\pi) - K(\tfrac{1}{4}\pi),$$

where E and K are complete elliptic integrals.

5. The hyperbolic case ($P > 0$)

Writing now
$$P^{\frac{1}{4}} = N > 0, \tag{5.1}$$

we have when $A > 0$
$$t = \pm \int_A^\infty \frac{dA}{A^2(1+N^4A^4)^{\frac{1}{2}}}, \tag{5.2}$$

the constant of integration again being suitably chosen. The substitution

$$NA = \cot(\tfrac{1}{2}\beta) \tag{5.3}$$

reduces (5.2) to
$$t = \pm \tfrac{1}{2}N \int_0^\beta \frac{\tan^2(\frac{1}{2}\beta)\, d\beta}{(1-\frac{1}{2}\sin^2\beta)^{\frac{1}{2}}} \tag{5.4}$$

and hence

$$t = \pm N[\tan(\tfrac{1}{2}\beta)(1-\tfrac{1}{2}\sin^2\beta)^{\frac{1}{2}} - E(\beta, 1/2^{\frac{1}{2}}) + \tfrac{1}{2}F(\beta, 1/2^{\frac{1}{2}})], \tag{5.5}$$

where E and F are given by (4.5).

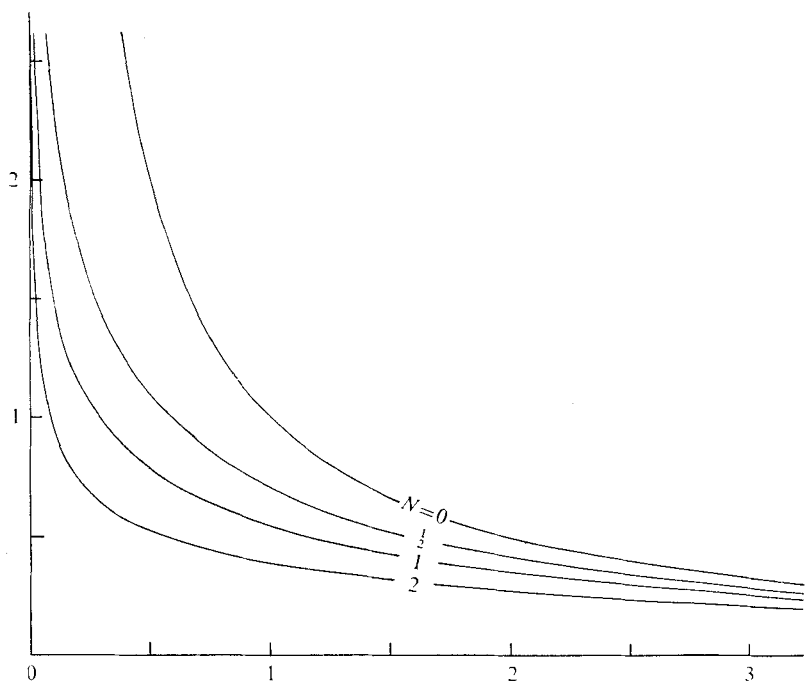

FIGURE 4. The function A when $P > 0$, giving the velocity at a fixed point as a function of t. The curves for $A < 0$ and $t < 0$ may be obtained by reflexion in the axes.

As before, A may now be plotted as a function of t (see figure 4). The curves for $A > 0$, $t > 0$ may be extended by reflexion in either the t axis or the A axis. A new feature, which did not appear in figure 2, is the presence of a singularity at $t = 0$. In the neighbourhood of this point we have from (5.2)

$$t \sim \pm (3N^2A^3)^{-1}, \quad NA \sim \pm (N/3t)^{\frac{1}{3}}. \tag{5.6}$$

Thus the velocity (except at $x = y = 0$) becomes infinite like $t^{-\frac{1}{3}}$ and the pressure (except at the free surface) like $t^{-\frac{4}{3}}$. The *displacement* near $t = 0$ is like the integral of the velocity and remains finite.

As we saw earlier, the cross-section of the free surface is a hyperbola, given by

$$(\dot{A} + A^2)\, x^2 - (\dot{A} - A^2)\, y^2 = QA^4. \tag{5.7}$$

Since in this case $\dot{A}^2 > A^4$ it follows that the coefficients of x^2 and y^2 have the same signs as $\dot{A}$ and $-\dot{A}$ respectively. We may distinguish three cases as follows.

Case 1: $Q > 0$

Then if $\dot{A} > 0$ the form of the free surface is as shown in figure 5 (a), the shaded area indicating the region where the pressure is positive. The angle which the asymptotes make with the x axis, namely

$$\alpha = \arctan \left(\frac{\dot{A} + A^2}{\dot{A} - A^2}\right)^{\frac{1}{2}}, \tag{5.8}$$

is greater than 45°. The angle decreases or increases according as $A \gtrless 0$. The semi-axis a of the hyperbola is given by

$$a^2 = QA^4/(\dot{A} + A^2). \tag{5.9}$$

As $t \to 0$ we have asymptotically

$$a^2 \sim QA^4/\dot{A} \sim Q/P^{\frac{1}{2}}. \tag{5.10}$$

If, on the other hand, $\dot{A} < 0$ the form of the free surface is as shown in figure 5 (b). The angle α is less than 45°, and the semi-axis b is given by

$$b^2 = QA^4/(-\dot{A} + A^2). \tag{5.11}$$

Basically (and in the absence of gravity) the configuration is the same as in figure 5 (a) but turned through a right-angle.

Case 2: $Q < 0$

Then if $\dot{A} > 0$ the form of the free surface is as in figure 6 (a), the angle α being greater than 45°. The shading shows the region of positive pressure. If $\dot{A} < 0$ the configuration is as in figure 6 (b).

Case 3: $Q = 0$

In this case the free surface reduces to two planes making equal angles $\pm\alpha$ with the x axis. If $\dot{A} > 0$ the configuration is as in figure 7 (a), and if $\dot{A} < 0$ as in figure 7 (b).

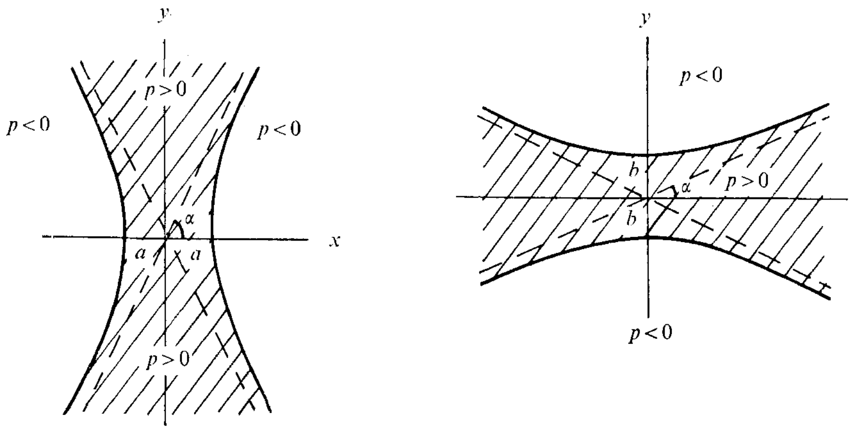

(a) (b)

FIGURE 5. The form of the free surface when $P > 0$ and $Q > 0$. (a) $\dot{A} > 0$, (b) $\dot{A} < 0$.

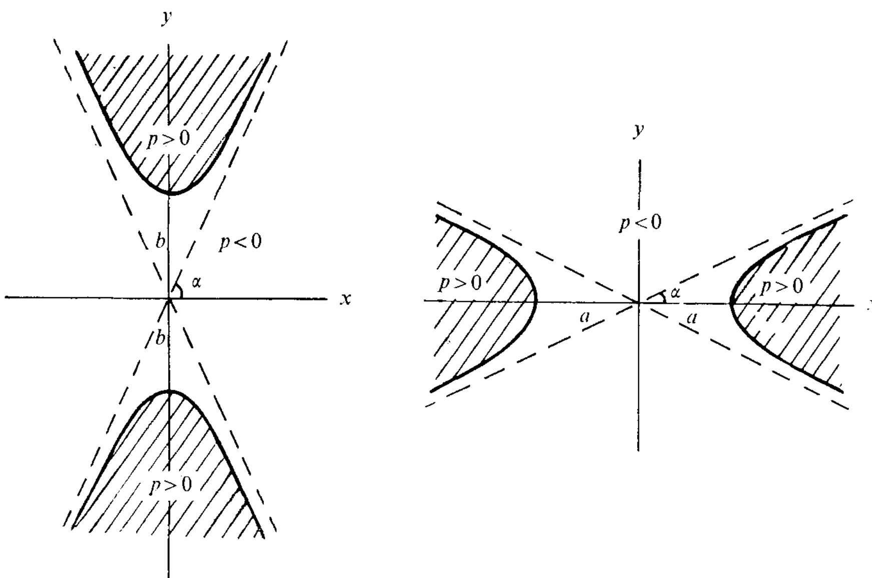

(a) (b

FIGURE 6. The form of the free surface when $P > 0$ and $Q < 0$. (a) $\dot{A} > 0$, (b) $\dot{A} < 0$.

In the hyperbolic solutions just found, both pressure and velocity become large at infinity. Hence these are essentially *local* solutions, which may nevertheless describe the local behaviour of some realizable flows. For example the solution of figure 5(a) may describe the time-dependent behaviour of a jet impinging on a plane surface ($y = 0$). The flow of figure 6 may partially describe the collapse of a mound of fluid under gravity. In each case the existence of a singularity at $\alpha = 45°$ is very interesting. It appears that as this angle is approached a weak shock will occur and that the pressure gradient will change sign. Thus the configuration of figure 5(a) will go over into the configuration of figure 6(b) (and that of figure 6(a) into that of figure 5(b)). Where the pressure

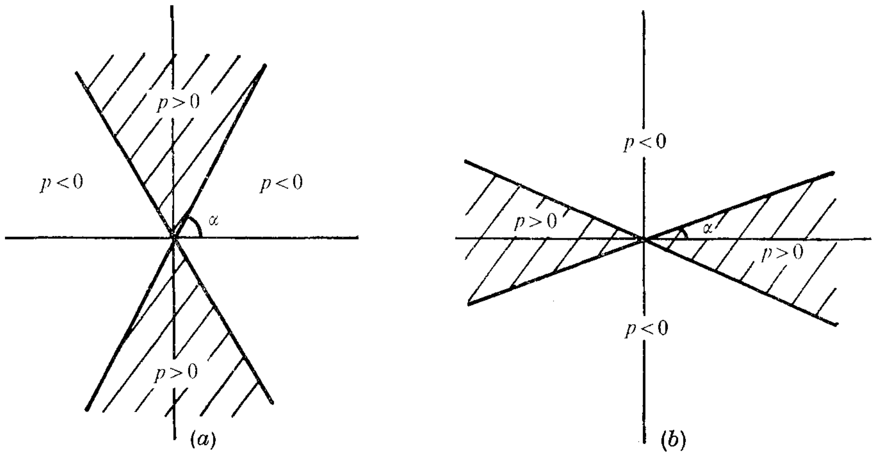

FIGURE 7. The form of the free surface when $P > 0$ and $Q = 0$. (a) $\dot{A} > 0$, (b) $\dot{A} < 0$.

was previously positive it now becomes negative, and a flow that was stable becomes suddenly unstable.

It is natural to consider how these solutions are related to the problem of the limiting form of a standing gravity wave of maximum amplitude. Penney & Price (1952) showed that at the instant of maximum elevation the acceleration at the crest of a standing wave is equal to g, directed downwards. Thus the fluid near the crest is in a state of almost free fall. Penney & Price suggested on theoretical grounds that the limiting slope at the crest should be 45°. These authors' arguments were not accepted by Taylor (1953), who nevertheless showed experimentally that the maximum slope was indeed very close to 45°. However, the occurrence of instabilities near the crest made the precise observation of the maximum angle rather difficult.

Since the hyperbolic solution described above has a singularity at $t = 0$, at which the velocity becomes infinite, it evidently does not describe the motion in a smooth standing wave. Nevertheless, since the fluid near the crest is in a state of almost free fall, the flows of figures 5 (b) and 7 (b) (in the region $p < 0$) may well represent possible instabilities that could occur near the instant of maximum elevation.

6. The intermediate case ($P = 0$)

In this special case (3.9) becomes

$$t = \pm 1/A. \tag{6.1}$$

Let us suppose, without loss of generality, that $A > 0$. Then we have two possibilities. If

$$t = 1/A \tag{6.2}$$

we have from (3.12)

$$\frac{p}{\rho} = -\frac{y^2}{t^2} + \frac{Q}{2t^4}. \tag{6.3}$$

Then the free surface $p = 0$ is given by

$$|y| = (\tfrac{1}{2}Q)^{\frac{1}{2}} t^{-2}. \tag{6.4}$$

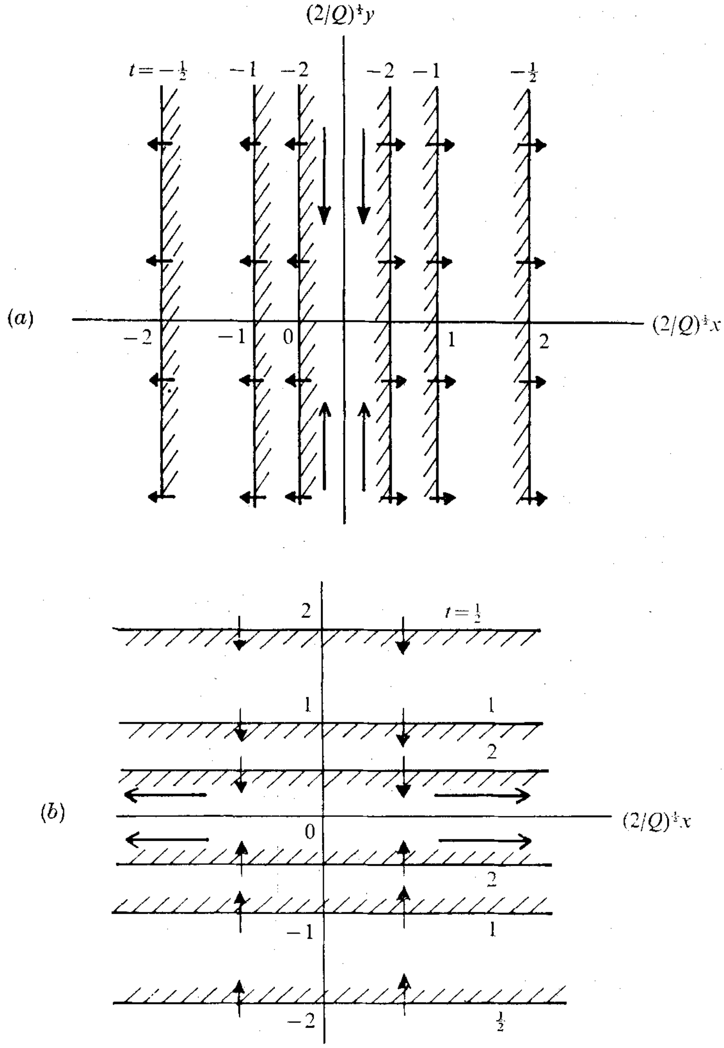

FIGURE 8. Successive configurations of the free surface when $P = 0$.

The flow is contained between two planes parallel to the x axis, which come together with velocity $(2Q)^{\frac{1}{2}}t^{-3}$ (see figure 8(*b*)). The pressure on the x axis is proportional to t^{-4}. Hence as $t \to 0$ the pressure becomes very large, as a greater and greater thickness of fluid has to be accelerated outwards.

The second possibility, when $t = -1/A > 0$, is essentially the reverse of the first; the fluid is contained between two lines parallel to the y axis (figure 8(*a*)).

A paradoxical feature of the flow described by (6.2)–(6.4) is that although the horizontal pressure gradient is zero the horizontal velocity u given by (3.2) appears at first sight to be decelerating (since $A \propto t^{-1}$). The paradox is resolved by recognizing the difference between the Eulerian acceleration $\partial u/\partial t$ and the Lagrangian acceleration Du/Dt. In fact any *marked particle* moves outwards with constant horizontal velocity u (though with steadily diminishing vertical velocity v), so that the horizontal component of the Lagrangian acceleration vanishes everywhere.

The flow is such that when t is small all particles start from the neighbourhood of the line $x = 0$. As t increases, an observer at a fixed point sees first the swiftest particles, since they arrive first, then particles with gradually slower and slower velocities. Hence to a fixed observer the velocity appears to be decreasing in time. The flow is analogous to an expanding universe.

An experiment to test the reality of this flow will be described in § 8.

The flow will be recognized as being related to a well-known channel flow, based on the nonlinear shallow-water theory in which vertical accelerations are neglected (see, for example, Forchheimer 1930). The present solution is however exact, and is independent of the shallow-water approximation.

7. Particle trajectories

The Lagrangian description of the class of flows described in this paper is almost as simple as the Eulerian. Thus let (X, Y) denote the co-ordinates of a fixed particle, functions of the time t and of the initial positions (X_0, Y_0) of the particle at time t_0. Then corresponding to the flow described by (3.1) we have

$$\left.\begin{aligned} dX/dt &= u = \partial\phi/\partial x = Ax = AX, \\ dY/dt &= v = \partial\phi/\partial y = -Ay = -AY, \end{aligned}\right\} \tag{7.1}$$

and so

$$\frac{1}{X}\frac{dX}{dt} = A(t), \quad \frac{1}{Y}\frac{dY}{dt} = -A(t). \tag{7.2}$$

Hence

$$X = X_0 F(t), \quad Y = Y_0/F(t), \tag{7.3}$$

where

$$F(t) = \exp\left[\int_{t_0}^{t} A\, dt\right]. \tag{7.4}$$

It can be shown directly that an expression of the general form (7.3) satisfies the Lagrangian equations of continuity and of motion, and that the pressure is constant on a free surface of elliptical cross-section provided that

$$F\ddot{F} = \lambda F^{-1} d^2(F^{-1})/dt^2, \tag{7.5}$$

λ being a constant related to the axes of the ellipse.

The special flow described in § 6 corresponds to

$$A = 1/t, \quad F = t_0/t. \tag{7.6}$$

The pressure in this case is given by

$$p = \tfrac{1}{2}(h_0^2 - Y_0^2)\, t_0^2/t^2,$$

where h_0 denotes the total depth of water at time t_0.

8. Experimental verification

In order to neutralize the effects of gravity on these free-surface flows there are at least three experimental alternatives.

(1) The experiments may be conducted under conditions of free fall. This was in effect the method adopted by Taylor (1960), who replaced the time variation by a gradual space variation, in a free nearly two-dimensional jet.

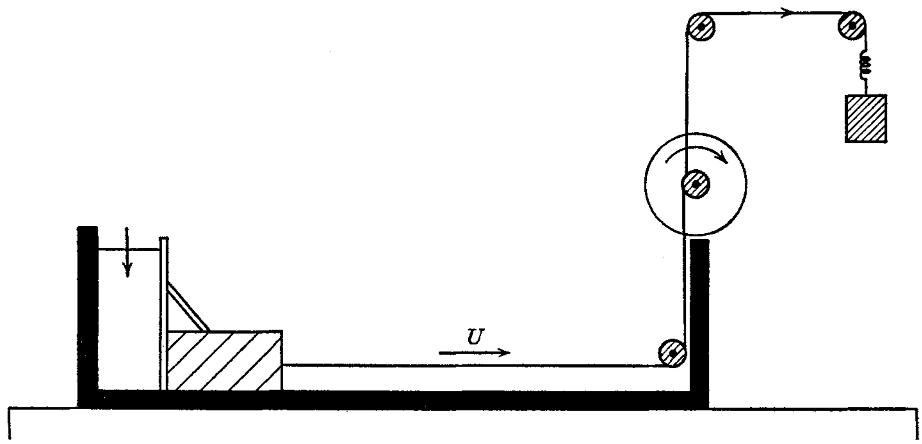

FIGURE 9. Sketch of apparatus to generate the free-surface flow corresponding to $Q = 0$.

(2) The experiments may be conducted at high speed or on a small scale, so as to increase the Froude number and reduce the effective value of g. A limit to the reduction in scale is set by surface tension. Thus high speed appears the more promising.

(3) In some configurations gravity may be counterbalanced by a hydrostatic pressure gradient. For this to be possible the free surface must be horizontal. The only instance is when $P = 0$ (§ 6).

This suggested the following simple experiment.

Let a rectangular tank be fitted with a movable block, which initially is near one end of the tank, as in figure 9. Let the space between the block and that end of the tank be filled with a volume Ω of water initially at rest. At time t_0 let the block be quickly accelerated to a uniform velocity U, say, along the tank. The water should then follow the plunger in such a way that the free surface remains horizontal and the depth of water in the tank is given by

$$h = \Omega/Ut. \tag{8.1}$$

The horizontal component of velocity in the tank will be given by

$$u = Ux/x_B, \tag{8.2}$$

where x is the distance from one end of the tank and $x_B = Ut$ is the distance through which the block has travelled. Thus we have $u = Ax$ as in (3.2), since $A = 1/t$.

Any other motion of the plunger will cause a tilting of the free surface – for example if the plunger is accelerated or decelerated, or if it is suddenly removed altogether as in the collapse of a dam. Such flows will invite specifically gravitational effects.

Figure 10 (plates 1 and 2) shows the realization of such an experiment in a rectangular tank of height 18 in., width $10\frac{1}{2}$ in. and total length 12 ft 2 in. The block, which moves from right to left, is in the form of a trolley running on rubber wheels. Attached to the rear of the trolley is a vertical sheet of plywood, sealed to the floor and side walls of the tank by a thin rubber sheet. Attached to the front of the trolley is a sponge-rubber buffer and a horizontal steel cable, which in turn is attached to an electric motor, as in figure 9. When the trolley reaches the far end of the tank the clutch is automatically released and the trolley comes to an abrupt halt. The trolley also carried two bricks whose weight helped to seal the lower edge of the rubber sheet to the floor of the tank.

At the start of the experiment the trolley was held in position by a long pole (whose shadow on the rear wall is visible to the left of the trolley in figure 10) while the space to the right of the trolley was filled with dyed water, to a height of 14 in. At the word 'go' the pole was released and the clutch of the motor was engaged. The trolley quickly accelerated to an almost uniform speed of about 1·5 ft/s. The sequence of photographs in figure 10 was taken with a cine camera running at 64 frames/s. A selection of frames is shown, the serial numbers of each frame being given on the right.

It can be seen that, at the start of the run, the initial acceleration of the trolley produces a tilt of the free surface, and hence an incipient wave (figures 10 (*a*)–(*c*), plate 1). But as the motion of the trolley becomes more uniform the wave is damped out and the surface becomes level to a remarkable degree (figures 10(*h*)–(*j*), plate 2).

On reaching the far end of the tank the trolley comes to a halt and water begins to pile up against the rear face of the trolley (figures 10 (*k*) and (*l*), plate 2). Fluid is then thrown back (figures 10 (*m*) and (*n*), plate 2) on top of the horizontal stream, which continues to flow from right to left and to diminish in depth. At this stage, and indeed after about figure 10 (*e*) (plate 1), the horizontal flow is supercritical, that is to say the velocity u exceeds $(gh)^{\frac{1}{2}}$, and hence the oncoming stream remains unaffected by the return flow. At a later stage (not shown in figure 10) a bore is formed travelling from left to right. Ultimately, viscosity and turbulence damp the flow, but in the short time corresponding to figures 10 (*a*)–(*n*), the thickness of the boundary layer, given by $(\nu t)^{\frac{1}{2}}$, is of order 1 mm, and so can be neglected.

In principle it is possible to reverse the experiment and to compress the fluid by forcing the plunger in the opposite direction (towards the fixed end) still maintaining a horizontal free surface. But in practice the required initial flow would be difficult to establish. Any irregularity of the free surface would cause wave motion, and the horizontal contraction of the fluid by the plunger would then tend to increase the wave amplitude through work done against the radiation stresses (see Longuet-Higgins & Stewart 1961; Taylor 1962).

When, on the other hand, the plunger moves *away* from the fixed end, any unwanted disturbance of the free surface tends to be reduced.

Dr J. S. Turner kindly assisted me with the experiments described in § 8. I am indebted to Sir Geoffrey Taylor for interesting discussions.

REFERENCES

Byrd, P. F. & Friedman, M. D. 1954 *Handbook of Elliptic Integrals for Engineers and Physicists*. Springer.

Dirichlet, G. L. 1860 Untersuchungen über ein Problem der Hydrodynamik. *Abh. Kön. Gest. Wiss. Göttingen*, **8**, 3–42.

Forchheimer, P. 1930 *Hydraulik*. Leipzig: Teubuer.

Lamb, H. 1932 *Hydrodynamics*, 6th edn. Cambridge University Press.

Longuet-Higgins, M. S. 1969 The exact hydrodynamical description of a slosh. *Proc. NATO Advanced Study Institute on Topics in Geophys. Fluid Dyn.*, p. 44. Univ. Coll. N. Wales, Bangor.

Longuet-Higgins, M. S. & Stewart, R. W. 1961 The changes in amplitude of short gravity waves on steady non-uniform currents. *J. Fluid Mech.* **10**, 529–549.

Penney, W. G. & Price, A. T. 1952 Finite periodic stationary gravity waves in a perfect fluid. *Phil. Trans. Roy. Soc.* A **244**, 254–284.

Taylor, G. I. 1953 An experimental study of standing waves. *Proc. Roy. Soc.* A **218**, 44–59.

Taylor, G. I. 1960 Formation of thin flat sheets of water. *Proc. Roy. Soc.* A **259**, 1–17.

Taylor, G. I. 1962 Standing waves on a contracting or expanding current. *J. Fluid Mech.* **13**, 182–192.

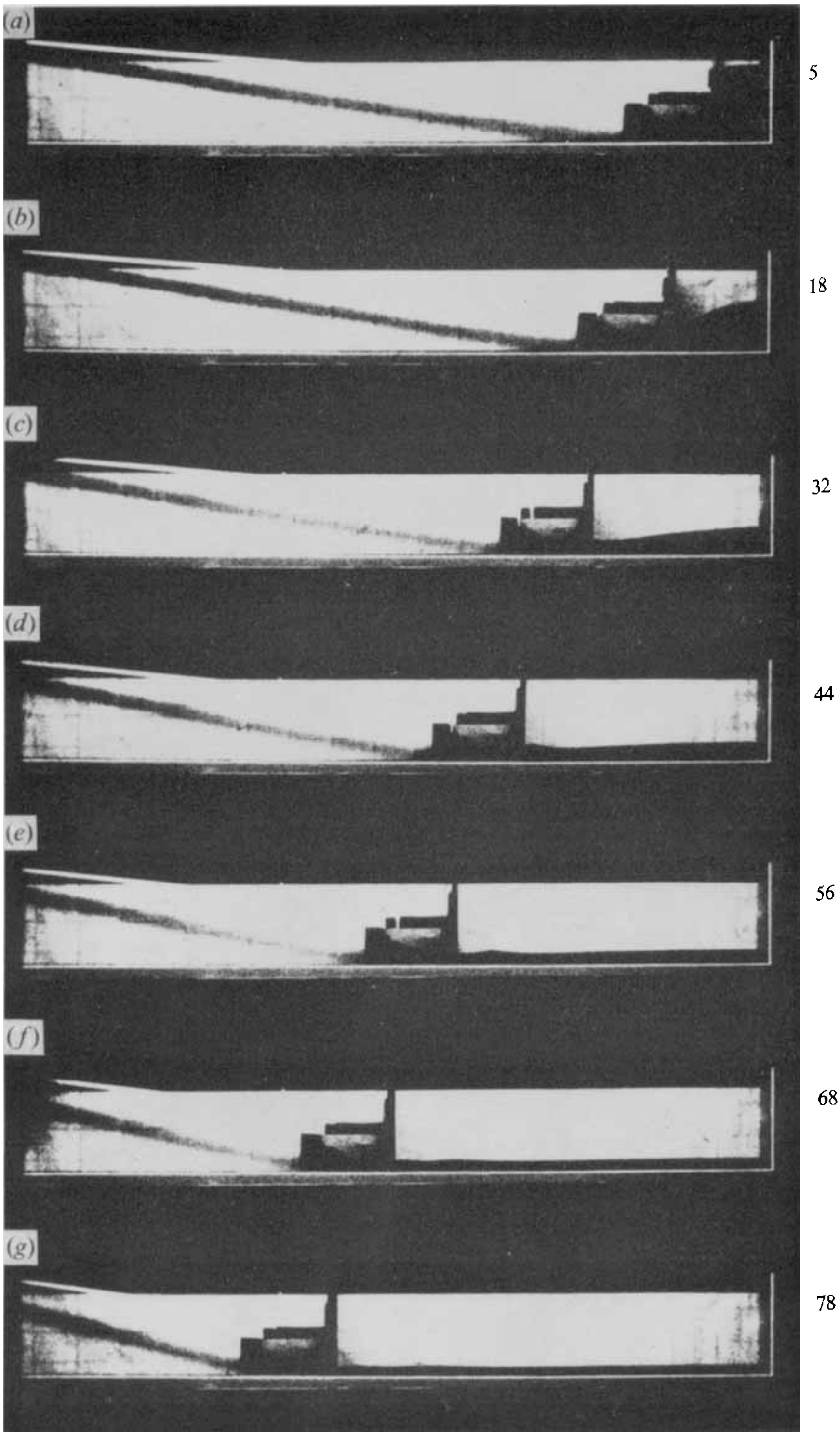

FIGURES 10 (*a*) to (*g*)

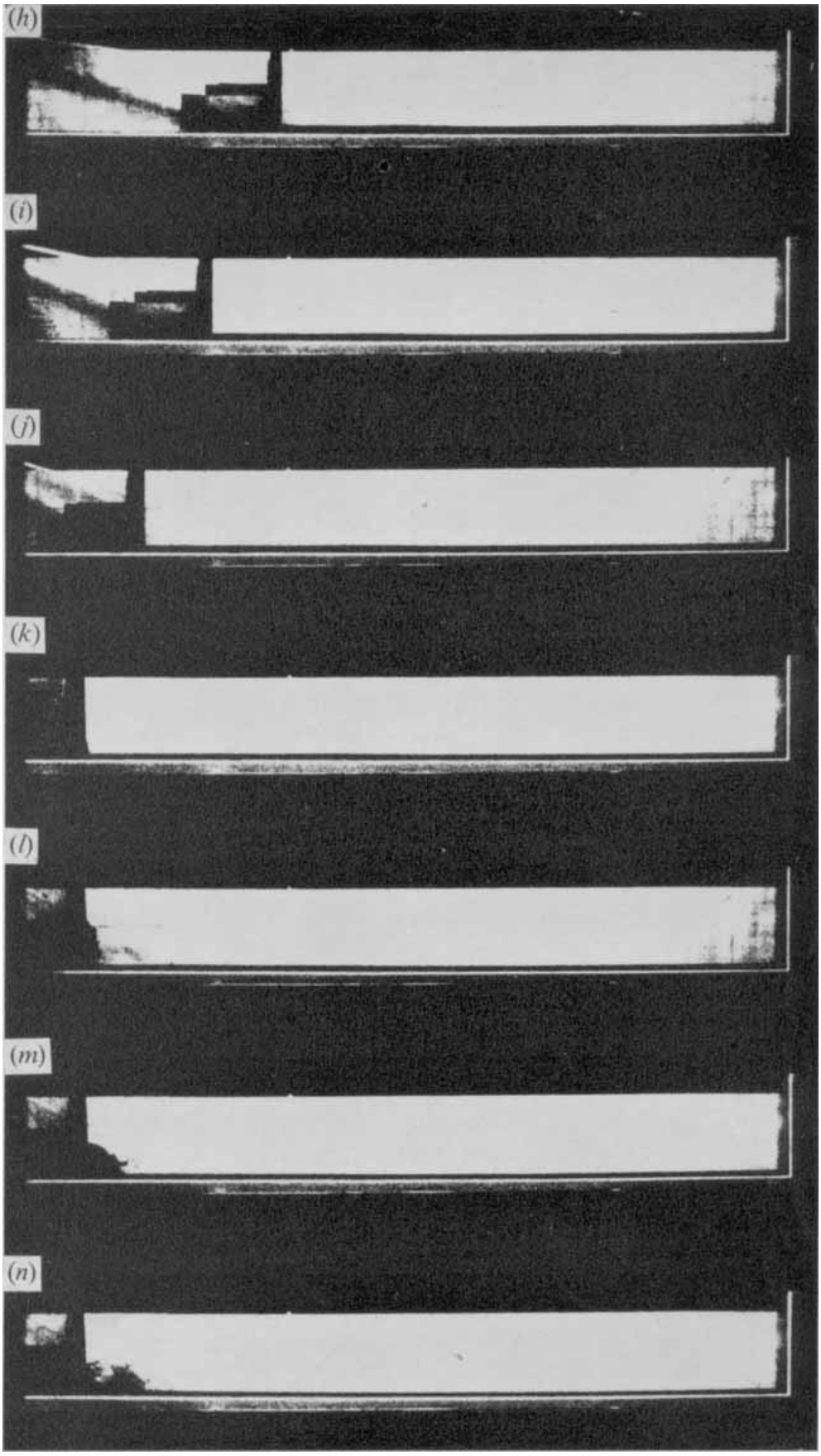

90

102

114

128

140

154

166

FIGURES 10 (*h*) to (*n*)

FIGURE 10. A model experiment designed to realize the expanding flow described in §6. Each number on the right indicates the serial number of the corresponding frame. The film was shot at 64 frames per second.